The Journal of Green Energy and Environmental Engineering

Research Paper

Synthesis of Water-Soluble Amphoteric Branched Polymer and Its Temperature and Salt Resistance Performance

Gabriel Wallner[1], Abdallah Granite[2,*]

[1] Acoustic Neuroimaging and Therapy Laboratory, Fondazione IRCCS Istituto Neurologico Carlo Besta, Milan, Italy
[2] Christian Doppler Laboratory for Superimposed Mechanical-Environmental Ageing of Polymeric Hybrid Laminates, University of Linz, Austria
*Corresponding author: Abdallahgranite@jku.at

Abstract. The water-soluble amphoteric branched polymers were synthesized by the copolymerization of acrylamide, 2-acrylamido-2-methylpropyl sulfonic acid with N-(3-acrylamidopropyl)trimethylammonium chloride using potassium persulfate and organic amine HMTEA as the initiator through the exothermic reaction system. The influence of synthetic factors was explored to give the optimal synthetic conditions. The structure and aggregation morphology of the copolymers were characterized by infrared spectroscopy, nuclear magnetic resonance spectroscopy, and electron microscopy. The characteristic viscosity of these copolymers was measured using the Ubbelohde viscometer and their molecular weights may be estimated. The viscous behavior of the copolymer solution was studied using a viscometer. The influence of various factors was explored. It was found that the polymer PAAA-1, when added at a polymer concentration of 1500 mg/L, had an apparent viscosity of 19.13 mPa·s at 85°C in a brine solution of 32868 mg/L mineralization. As the salt solution concentration or the temperature increased, the apparent viscosity of the polymer solution decreased. However, the water-soluble amphoteric branched polymers exhibited better salt and heat resistance than the di-component copolymer of acrylamide and 2-acrylamide-2-methylpropyl sulfonic acid.

Keywords: *polymers; synthesis; aqueous solution; viscosity; rheology*

Received on 15 Feb 2025, Accepted on 15 April 2025, Published on 15 May 2025

1 Introduction

The global energy landscape continues to rely heavily on hydrocarbon resources, even as the transition to renewable energy accelerates. In this context, maximizing the recovery from existing oil reservoirs has become a critical strategy for energy security and economic efficiency. Enhanced Oil Recovery (EOR) techniques are pivotal in this endeavor, aiming to mobilize the significant portion of crude oil (often 50-70% of Original Oil in Place, OOIP) that remains trapped after primary and secondary recovery methods . Among various EOR methods, chemical flooding, particularly polymer flooding, stands out due to its operational simplicity, cost-effectiveness, and proven field success, especially in major oil-producing regions like China . The fundamental principle of polymer flooding is to increase the viscosity of the injected aqueous phase, thereby improving the mobility ratio between the displacing fluid and the displaced crude oil. This leads to better volumetric sweep efficiency, reduced viscous fingering, and ultimately, higher incremental oil recovery .

Partially Hydrolyzed Polyacrylamide (HPAM) has been the industry workhorse for polymer flooding for decades, valued for its high molecular weight, effective thickening capability, and relatively low cost . However, the widespread application of HPAM faces severe limitations in reservoirs characterized by high temperature (typically > 80°C) and high salinity (Total Dissolved Solids, TDS > 30,000 ppm), conditions that are increasingly common as exploration and production move into more challenging geological formations . The performance degradation of HPAM under such harsh conditions is multifaceted. At elevated temperatures, the amide groups ($-CONH_2$) on the HPAM backbone are prone to hydrolysis, converting to carboxylate groups ($-COO^-$). This not only

alters the polymer's charge density but also, in the presence of divalent cations like Ca^{2+} and Mg^{2+} commonly found in formation brines, can lead to cross-linking, precipitation, and catastrophic, irreversible viscosity loss . Furthermore, high ionic strength screens the electrostatic repulsion between the negatively charged carboxylate groups, causing the polymer chains to coil and contract, drastically reducing their hydrodynamic volume and solution viscosity—a phenomenon known as the "polyelectrolyte effect" . This chain coiling also diminishes the polymer's viscoelasticity and its ability to effectively plug high-permeability channels for improved conformance control. Field experiences and simulation studies have confirmed that sustaining injectivity and maintaining target viscosity under high-salinity, high-temperature (HSHT) conditions remain significant operational hurdles, often rendering conventional HPAM economically unviable for such reservoirs .

In response to these challenges, extensive research has been directed toward developing next-generation water-soluble polymers with enhanced thermal stability and salt tolerance. The strategies can be broadly categorized into several molecular design approaches:

Incorporation of Functional Monomers: Copolymerizing acrylamide (AM) with monomers bearing sulfonate groups, such as 2-acrylamido-2-methylpropanesulfonic acid (AMPS) or its salts, is a well-established method. The strong hydration shell and charge stability of the sulfonate group ($-SO_3^-$) provide superior shielding against multivalent cations and improve chain rigidity, significantly boosting salt tolerance . Monomers like N-vinylpyrrolidone (N-VP) are introduced to protect the amide groups from hydrolysis at high temperatures, thereby enhancing thermal stability .

Design of Amphoteric/Zwitterionic Polymers: This approach involves incorporating both anionic and cationic monomers into the same polymer chain. The resulting amphoteric or zwitterionic polymers exhibit unique "antipolyelectrolyte" behavior: in high-salinity environments, the screening of electrostatic attractions between oppositely charged groups on the chain leads to chain expansion and an increase in viscosity, which is the opposite of conventional polyelectrolytes . This intrinsic salt tolerance, coupled with strong hydration from both ionic species, also contributes to excellent thermal stability. Recent studies highlight zwitterionic polymers as promising alternatives to HPAM, demonstrating not only better viscosity retention under HSHT conditions but also higher recovery factors in coreflooding experiments due to combined polymer-thickening and surfactant-like interfacial activity .

Construction of Branched and Associating Structures: Moving beyond linear architectures, polymers with branched, comb-shaped, or hydrophobic associating structures can offer improved shear resistance and stability. Branching points and hydrophobic associations can act as reversible, physical cross-links that maintain a robust network structure even when individual chains are affected by heat or salt, leading to better viscosity retention and elastic properties . The use of specific initiator systems, such as redox pairs capable of multi-point initiation, is a key synthetic route to creating such controlled branched architectures.

Development of Hybrid and Composite Systems: An emerging frontier involves creating hybrid systems by combining polymers with nanoparticles (e.g., silica, cellulose nanocrystals) or other additives. The nanoparticles can interact with polymer chains through hydrogen bonding or electrostatic forces, acting as physical cross-linkers that reinforce the molecular network. This synergy can significantly enhance the thickening efficiency, thermal stability, and aging resistance of the base polymer solution under harsh conditions .

Exploration of Biopolymers: Natural polymers like xanthan gum, guar gum, and newly developed microbial polymers (e.g., Basil Seed Gum, FH polymer) are investigated as environmentally friendly alternatives. They often possess inherent shear-thinning behavior, good salt tolerance, and biodegradability. However, challenges related to cost, consistency, and stability at very high temperatures (>90°C) sometimes limit their application .

Within this vibrant research landscape, the synthesis of water-soluble amphoteric branched polymers represents a sophisticated strategy that integrates the benefits of zwitterionic chemistry with a robust macromolecular architecture. Ternary copolymers based on acrylamide (AM, nonionic), 2-acrylamido-2-methylpropanesulfonic acid (AMPS, anionic), and a cationic monomer like (3-acrylamidopropyl)trimethylammonium chloride (APTAC) have shown particular promise. Studies have demonstrated that such terpolymers can achieve high molecular weights and exhibit significant viscosifying effects in high-salinity brines, leading to substantial increases in oil

recovery factor (up to 23-28%) compared to brine flooding alone . The antipolyelectrolyte effect, where chain expansion occurs in salt solutions, is a key mechanism behind their performance .

Building upon these foundations, the research presented in this paper addresses the pressing need for high-performance EOR agents suitable for extreme reservoir conditions, such as those encountered in the high-temperature, high-salinity oilfields. The core innovation lies in the integrated design and adiabatic synthesis of a water-soluble, amphoteric, branched copolymer. Specifically, this work employs an efficient redox initiation system composed of potassium persulfate (KPS) and a multi-amine organic reductant (HMTTA) to drive the copolymerization of AM, AMPS, and APTAC. The choice of HMTTA is strategic, as its multi-tertiary amine structure is hypothesized to enable multi-point initiation, fostering the formation of a desirable branched topology rather than a simple linear chain. This branched architecture is anticipated to enhance not only the molecular weight but also the shear recovery and long-term stability of the polymer solution. Moreover, the synthesis is conducted via an adiabatic polymerization process. This method leverages the exothermicity of the reaction, which is particularly significant for concentrated monomer solutions, to drive the polymerization to high conversion. The adiabatic approach offers crucial practical advantages for potential industrial scale-up, as it provides inherent process control data (temperature profiles) and can be more energy-efficient compared to isothermal processes requiring external cooling for highly exothermic reactions.

Therefore, this study systematically investigates: (1) the optimization of synthesis parameters (temperature, pH, initiator ratio, cationic monomer content) to achieve the optimal branched structure; (2) comprehensive characterization of the copolymer's chemical structure and aggregation morphology using FTIR, NMR, SEM, and TEM; (3) detailed evaluation of its solution rheology, focusing on viscosity-concentration relationships, temperature/salt resistance, and shear recovery behavior under simulated reservoir conditions. The ultimate goal is to develop a polymer that maintains a target apparent viscosity (e.g., >15 mPa·s) at high temperature (85°C) and high salinity (~32,868 mg/L) at economically viable concentrations, thereby providing a viable chemical solution for unlocking trapped oil in some of the world's most challenging reservoirs..

2 Experimental Section

2.1 Experimental Materials

Acrylamide (AM) and 2-acrylamido-2-methylpropanesulfonic acid (AMPS), industrial grade, Shandong Baomo Chemical Co., Ltd.; N-(3-Acrylamidopropyl)trimethylammonium chloride (APTAC), AR, Shanghai Macklin Biochemical Technology Co., Ltd.; Potassium persulfate (KPS), AR, Sinopharm Chemical Reagent Co., Ltd.; Polyacrylamide with 20 million molecular weight, Shanghai Macklin Biochemical Technology Co., Ltd.; Ethanol, AR, Kangde Chemical Co., Ltd.; Organic amine reducing agent (HMTTA), AR, J&K Scientific Ltd. Mineralized water with 32863 mg/L salinity was prepared in-house, with salt composition: 31993 mg/L NaCl, 175 mg/L $MgCl_2$, 700 mg/L $CaCl_2$; Mineralized water with 58002 mg/L salinity was prepared in-house, with salt composition: 55560 mg/L NaCl, 1213 mg/L $MgCl_2$, 3429 mg/L $CaCl_2$.

2.2 Synthesis of Water-Soluble Amphoteric Branched Copolymer

A certain amount of 2-acrylamido-2-methylpropanesulfonic acid (AMPS) and acrylamide (AM) were fully dissolved in an appropriate amount of deionized water. The pH was adjusted to 6-8 using sodium hydroxide. A certain amount of N-(3-acrylamidopropyl)trimethylammonium chloride (APTAC) was added, followed by the oxidant potassium persulfate. Deionized water was then added to reach a fixed solid content. After reaching the set temperature, the mixture was placed in a thermal insulation device. Under sealed conditions, nitrogen was purged for 30 minutes. The reducing agent HMTTA was then added dropwise to the reaction system via a syringe, and nitrogen purging continued for another 30 minutes. The ratio of oxidant to reducing agent in the initiator system was controlled, and the adiabatic reaction proceeded. The reaction was stopped when it formed a gel. The resulting product was crushed in ethanol, soaked, and then placed in a vacuum drying oven at 60°C for 2 hours, finally obtaining a white product. The synthesis process is shown in Fig. 1.

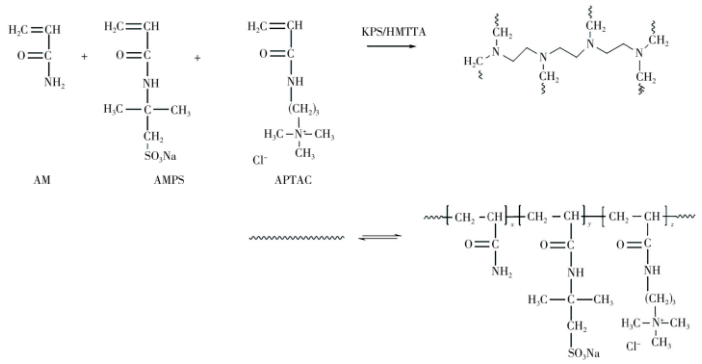

Figure 1 Synthesis process of water-soluble amphiphilic branched copolymer

2.3 Structural Characterization and Performance Testing Methods

2.3.1 ^{1}H Nuclear Magnetic Resonance (^{1}H NMR)

The product structure was characterized using a German Bruker AVANCE 400 MHz superconducting NMR spectrometer. An appropriate amount of the sample was dissolved in deuterated solvent. The solution was added to an NMR tube and placed in the NMR spectrometer for testing. The internal standard was tetramethylsilane. The NMR frequency was 500 MHz, and the test temperature was stabilized at 25°C.

2.3.2 Fourier Transform Infrared Spectroscopy (FTIR)

A German Bruker Tensor 27 FTIR spectrometer was used. An appropriate amount of the synthesized product was mixed with potassium bromide crystals at a mass ratio of (1:100) to (1:50) in a mortar, ground evenly, and pressed into a pellet. The pellet was placed in the FTIR spectrometer for testing. The scanning range was 4000-400 cm^{-1}, and the test temperature was stabilized at 25°C.

2.3.3 Apparent Viscosity Test

A Brookfield DV-II viscometer was used to measure the apparent viscosity of the samples. At room temperature (25°C), with the rotor shear rate set to 7.34 s^{-1} and test duration of 1 minute, the apparent viscosity of polymer samples at different concentrations in mineralized water or deionized water was measured. Rheological performance was tested using a HAAKE MARS 60 rotational rheometer with a CC24Ti measuring system to determine solution viscosity. The shear rate was 7.34 s^{-1}, and temperature-viscosity curves were measured for solutions prepared with different salt solutions or mineralized water at different temperature gradients. Using the same rotor, the shear rate was alternated between 7.34 s^{-1} and 100 s^{-1} to investigate the effect of shear rate on solution viscosity.

2.3.4 Scanning Electron Microscopy (SEM)

A Zeiss G300 scanning electron microscope was used. The aqueous solution and mineralized water solution of the sample were freeze-dried separately, coated with platinum, and then observed under the transmission electron microscope.

2.3.5 Transmission Electron Microscopy (TEM)

A Hitachi HT-7700 transmission electron microscope was used. Drops of the sample's aqueous solution or mineralized water solution were placed on a silicon wafer surface, dried under an infrared lamp, and then observed under the TEM.

2.3.6 Intrinsic Viscosity Measurement

The Ubbelohde viscometer was fixed in a constant-temperature water bath at 30°C with continuous stirring. The flow times for the blank solution and the test solution were measured and recorded. Each concentration was tested three times, with an error not exceeding 0.5 seconds. According to Q/SHCG 0159-2021 "Technical

Requirements for Oil Displacement Polyacrylamide", the intrinsic viscosity of the PAAA series polymers was determined using the Ubbelohde viscometer with an initial solution concentration of c = 500 mg/L, and the viscosity-average molecular weight of the polymers was calculated, where α is 0.66 and K is 3.73×10^{-2}.

3 Results and Discussion

3.1 Polymer Synthesis and Conditions

3.1.1 Effect of Temperature on the Reaction

The monomer mass ratio was fixed at 20%, initiator dosage at 0.02% of total monomer mass, mass ratio of AM:AMPS:APTAC at 60:40:1, and pH at 7. The effect of reaction temperature on polymerization was explored. Fig. 2(a) shows the real-time temperature recording curves for initiation at different starting temperatures. Lower starting temperatures resulted in slower reaction rates and longer times for complete reaction. Higher starting temperatures led to faster reaction rates and shorter completion times. A high starting temperature causes a sharp increase in the number of active free radicals in the system, increasing reaction activity and the chain termination rate, thus accelerating the reaction but lowering molecular weight and viscosity. However, if the temperature is too low, the polymerization reaction is incomplete, and a complete gel block cannot be obtained. Therefore, the reaction cannot be conducted at too low a temperature either. Fig. 2(b) shows the apparent viscosity of 2 g/L polymer solutions prepared in mineralized water with salinities of 58002 mg/L and 32868 mg/L for polymers synthesized at different initiation temperatures. The apparent viscosity gradually decreased as the polymerization temperature increased. The 14°C used in the experiment was the minimum temperature for complete polymerization. Subsequent reactions were conducted at 14°C.

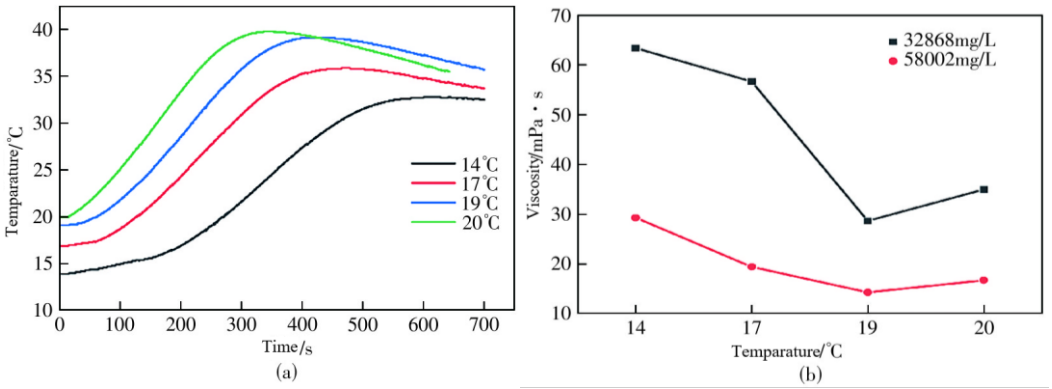

Figure 2 Real-time temperature recording curves during different temperature inducements and the apparent viscosity of the polymer in 2g/L mineralized water at different temperatures

3.1.2 Effect of pH on the Polymerization Reaction

In polymerization reactions, the pH of the reaction system can also affect the structure and properties of the polymer. When using a redox initiator system to synthesize polymers, monomer activity is noticeably affected by pH. The total monomer solid content was fixed at 20%, initiator dosage at 0.02% of total monomer mass, mass ratio of AM:AMPS:APTAC at 60:40:1, and the effect of reaction temperature on polymerization was explored with an initiation temperature of 14°C. The results are shown in Fig. 3. Within the pH range of 5-9, the copolymer obtained at pH=7 had the highest apparent viscosity. Furthermore, as observed from the real-time temperature recording curves for initiation at different pH values in Fig. 3(a), the reaction speed was faster at lower pH during polymerization, which is not conducive to forming polymers with higher molecular weight. In alkaline environments, the polymerization rate gradually slowed, significantly reducing reaction efficiency. Therefore, the optimal pH for the polymerization reaction system was selected as 7.

DOI:

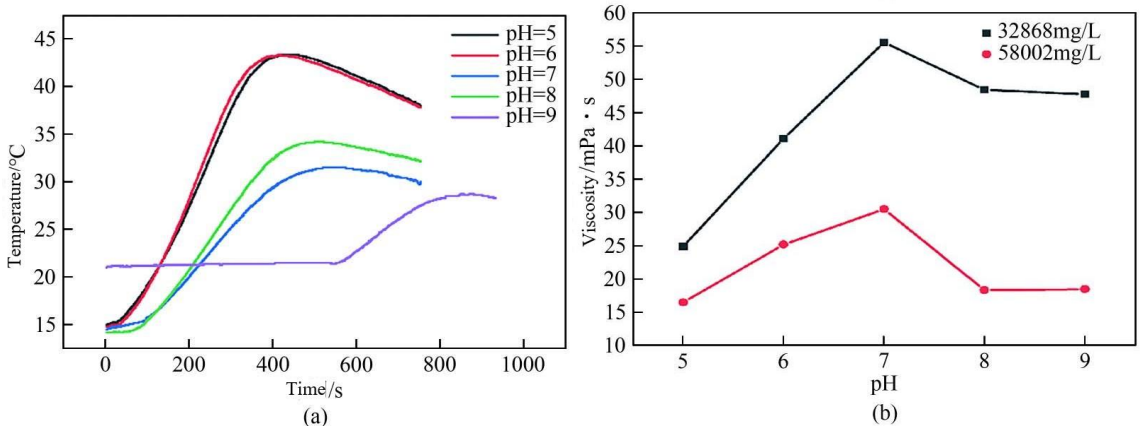

Figure 3 Real-time temperature recording curves during initiation at different pH values, and apparent viscosity of polymer product with a dosage of 2g/L in mineralized water at different pH values

3.1.3 Effect of Oxidant to Reductant Ratio on the Reaction

The molar ratio of oxidant to reductant in the initiator is also an important factor affecting the reaction. Correctly controlling the mass ratio of oxidant and reductant is crucial for improving reaction efficiency and yield. To determine the optimal mass ratio of oxidant and reductant, calculations can be made based on molar mass and molar ratio. The total monomer solid content was fixed at 20%, mass ratio of AM:AMPS:APTAC at 60:40:1, pH at 7, starting temperature at 14°C, and the molar ratio of oxidant to reductant in the initiator was controlled. The results are shown in Fig. 4. It was found that the polymerization product performed best when the reductant was slightly in excess. This is estimated to be because the reductant in the initiation system has a multi-tertiary amine structure, allowing multi-point initiation to form a branched structure during the initiation process. Possibly, the reactivity of the methyl groups on the tertiary amine differs during initiation, requiring the addition of more reductant. Therefore, subsequent reactions used an oxidant to reductant ratio of 1:1.2.

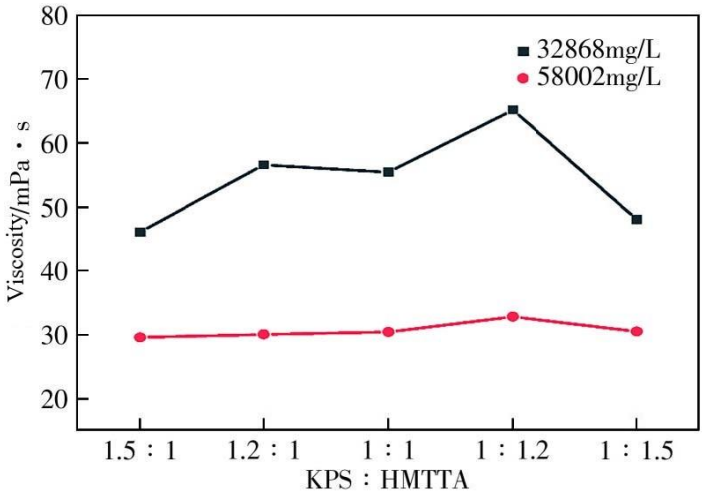

Figure 4 Effect of different molar ratios of oxidant to reducing agent on the apparent viscosity of mineralized water with a polymer dosage of 2g/L

3.1.4 Effect of Cationic Monomer Dosage

The total monomer mass ratio was fixed at 20%, mass ratio of AM:AMPS at 60:40, pH at 7, reaction starting temperature at 14°C, initiator dosage at 0.02% of total monomer mass, oxidant to reductant molar ratio at 1:1.2. The effect of adding different mass fractions of APTAC on polymer solution viscosity was studied. The results are shown in Fig. 5. The mass fractions of APTAC added were 0, 1%, 2%, 5%, and 10%, yielding samples PAA-0, PAAA-1, PAAA-2, PAAA-5, and PAAA-10, respectively. It can be seen that as APTAC was added to the polymer system,

DOI:

the apparent viscosity of the polymer system first increased and then decreased. Adding a small amount of cationic monomer increased the polymer's viscosity, mainly because the side groups of the cationic monomer can form complex structures with sulfonate groups, or its counterions interact with hydrogen atoms on the amide group, leading to increased viscosity. However, adding too much reduces the polymer molecular weight, and these complex interactions intensify, causing the polymer chains to contract, leading to decreased viscosity. From Fig. 5, it is evident that the polymer system had the highest viscosity when the APTAC mass fraction was 1%.

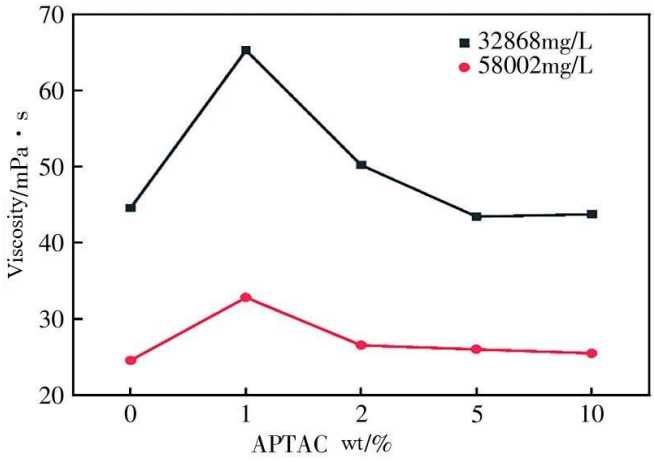

Figure 5 Effect of different APTAC dosages on the apparent viscosity of polymer solution (polymer dosage is 2g/L)

3.2 Structural Characterization of the Copolymers

Fig. 6 shows the FTIR spectra of the binary copolymer PAA-0 and the PAAA series polymers. Fig. 6(a) is the FTIR spectrum of sample PAAA-1. The characteristic absorption peaks at 1675 cm^{-1} and 3375 cm^{-1} can be identified as the -$CONH_2$ and -NH_2 bonds in the AM unit, respectively. The characteristic absorption of the S-O bond in the sulfonate group -SO_3^- of AMPS is at 1038 cm^{-1}. The characteristic absorption peak of the C=O bond in the AMPS unit is at 1195 cm^{-1}. The peak at 2972 cm^{-1} is the characteristic absorption of the methyl groups connected to N in APTAC. The above confirms the copolymerization of AM, AMPS, and APTAC, yielding a ternary copolymer product. The FTIR spectra of the binary copolymer PAA-0 and other polymers in the PAAA series are shown in Fig. 6(b). As the cationic monomer content increases, the characteristic absorption peak at 2972 cm^{-1} for the methyl groups connected to N in APTAC strengthens, confirming the successful synthesis of the PAAA series ternary copolymers.

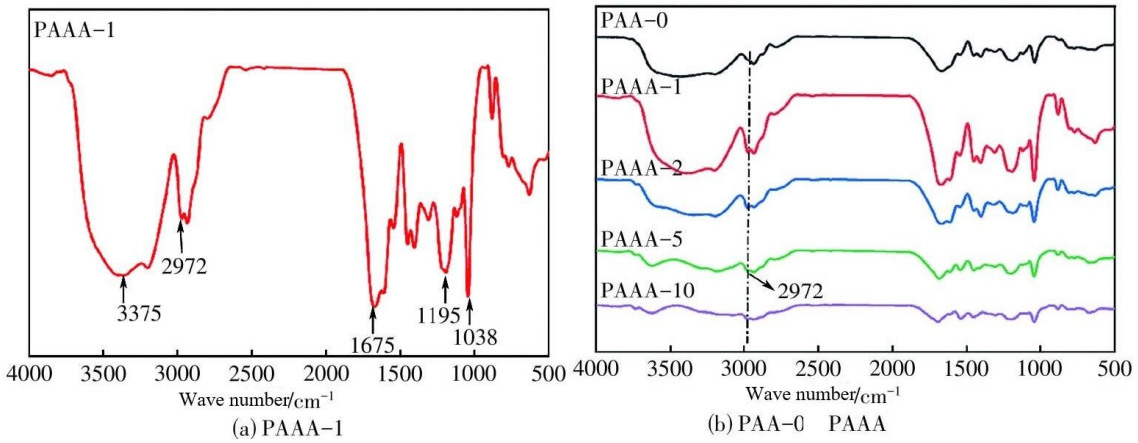

Figure 6 Infrared spectra of PAAA-1, PAA-0, and PAAA series polymers

Fig. 7 shows the ^1H NMR spectrum of the polymer. It can be seen that no absorption peaks for carbon-carbon

double bonds appear in the ^{1}H NMR spectrum, indicating that the monomers participated in the copolymerization reaction. The proton peak of the methylene group on the -CH_2SO_3Na group of AMPS appears at a chemical shift of 3.3-3.5 ppm. The proton peak of the -CH- group in the AMPS unit is at 1.5-1.6 ppm. Simultaneously, the proton peaks of the methine and methylene groups on the polymer backbone are at 2.1-2.3 ppm and 1.5-1.8 ppm, respectively. The proton peak of the methyl groups connected to N in APTAC is at 3.0-3.2 ppm. The ^{1}H NMR spectra of other polymers in the PAAA series are shown in Fig. 7(b). It can be seen that the methyl peak at 3.0-3.2 ppm gradually increases with the amount of the third monomer, confirming the successful synthesis of the PAAA series ternary copolymers.

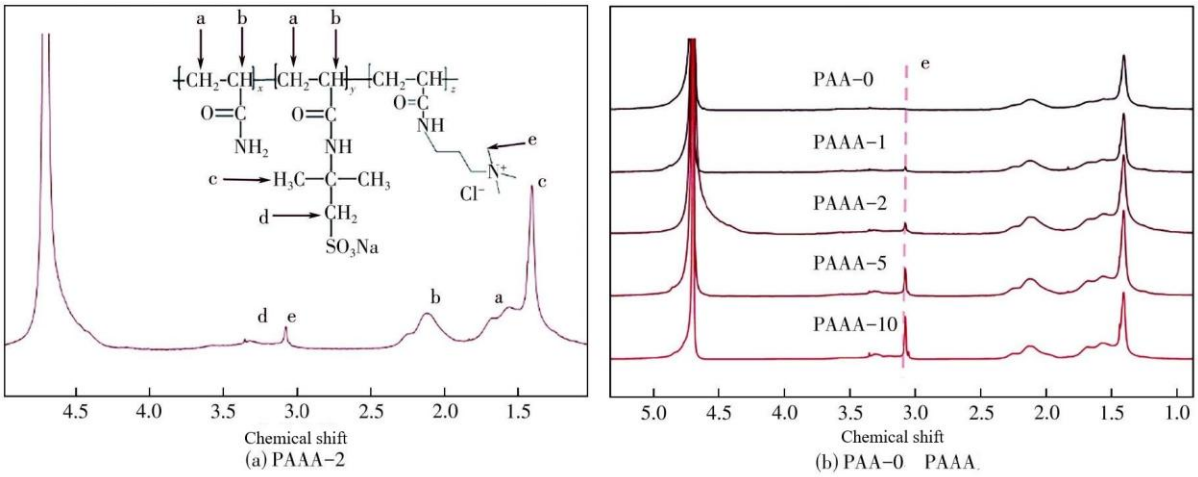

Figure 7 Nuclear magnetic resonance hydrogen spectrum of PAAA-2, PAA-0, and PAAA series polymers

Table 1 shows the intrinsic viscosity measurement results for the polymer systems. From the experimental data in Table 1, it is evident that the intrinsic viscosity of the ternary branched copolymer PAAA-1 is significantly higher than that of the binary copolymer PAA-0, reaching 3041 mL/g. Its calculated molecular weight reaches 27.58 million. The introduction of APTAC significantly increased the polymer molecular weight, indicating that the APTAC monomer effectively enhanced the polymer molecular weight by increasing chain rigidity and hydrophilicity, thereby increasing the viscosity of the polymer solution. As the content of the third monomer APTAC increases, the intrinsic viscosities of PAAA-2, PAAA-5, and PAAA-10 gradually decrease, and molecular weights also decrease. This indicates that the viscosity-increasing effect of the polymer does not necessarily increase linearly with increasing APTAC content. Especially when APTAC content is too high, the spatial structure of the polymer chains may change. Excessive cationic groups may lead to complexation between polymer chains, affecting the free movement and extension of molecular chains, resulting in decreased molecular weight, manifested as a reduction in intrinsic viscosity. An appropriate amount of APTAC monomer can promote interactions between polymer chains, increasing their viscosity and molecular weight, but excessive APTAC monomer adversely affects the polymer's structure and properties.

Table 1 Intrinsic Viscosity and Viscosity-Average Molecular Weight of PAAA Series Polymers

Sample Code	Intrinsic Viscosity / $mL \cdot g^{-1}$	Viscosity-Average Molecular Weight / 10^4
PAA-0	2842	2489
PAAA-1	3041	2758
PAAA-2	2649	2247
PAAA-5	2422	1954
PAAA-10	2369	1889

3.3 Aggregation Morphology of Copolymers

Fig. 8 shows transmission electron microscopy (TEM) images of 2000 mg/L PAA-0 and PAAA-1 solutions in 32868

mg/L mineralized water. From the TEM image of PAA-0 polymer in Fig. 8(a), it can be seen that the polymer coils up due to the presence of salt solution, forming a loose network structure. This is mainly because this acrylamide and 2-acrylamido-2-methylpropanesulfonate polymer is anionic; the high content of sulfonate negative charges repel each other, resulting in a loose structure. From the TEM image of the ternary copolymer PAAA-1 in Fig. 8(b), it can be seen that due to complexation between the third monomer APTAC at very low concentration and the sulfonate groups on the polymer chains, along with hydrogen bonding between the chloride ions on the quaternary ammonium and the amide bonds, a network structure is formed. In mineralized water, this network structure is denser than that of the binary copolymer, macroscopically manifesting as superior apparent viscosity compared to the binary copolymer.

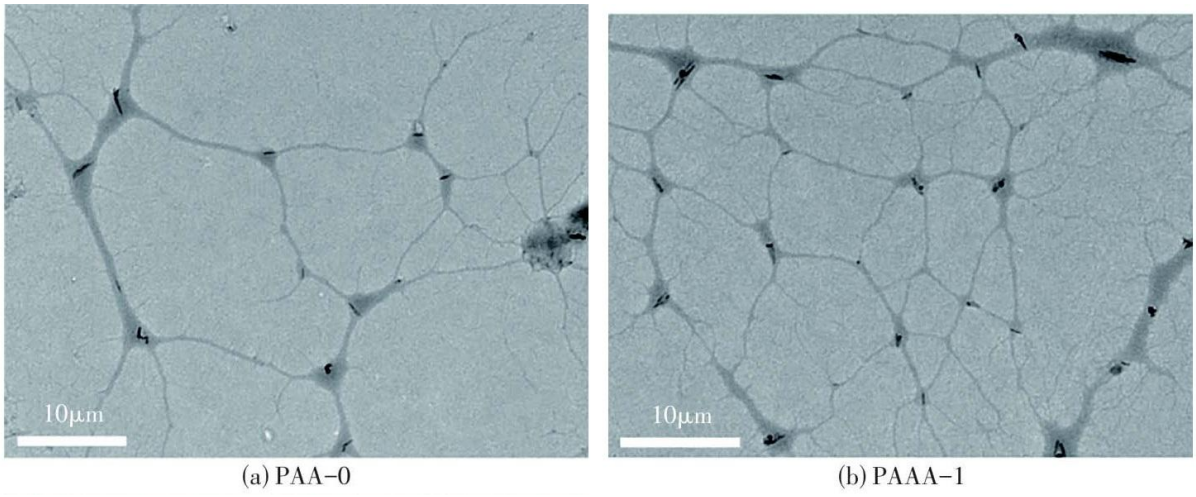

Figure 8 TEM images of PAA-0 and PAAA-1 in a 32868mg/L mineralized aqueous solution

Fig. 9 shows scanning electron microscopy (SEM) images of a 2000 mg/L polymer PAAA-1 solution in pure water and in 32868 mg/L mineralized water after freeze-drying. As seen from the figure, in pure water, the polymer exhibits a rich network structure, which can effectively increase the viscosity of the polymer solution. In mineralized water, due to the effect of salt on the polymer, the solution viscosity decreases. In the SEM images, the surface structure appears relatively dense, and filamentous polymer strands are seen in the pores left by salt particles.

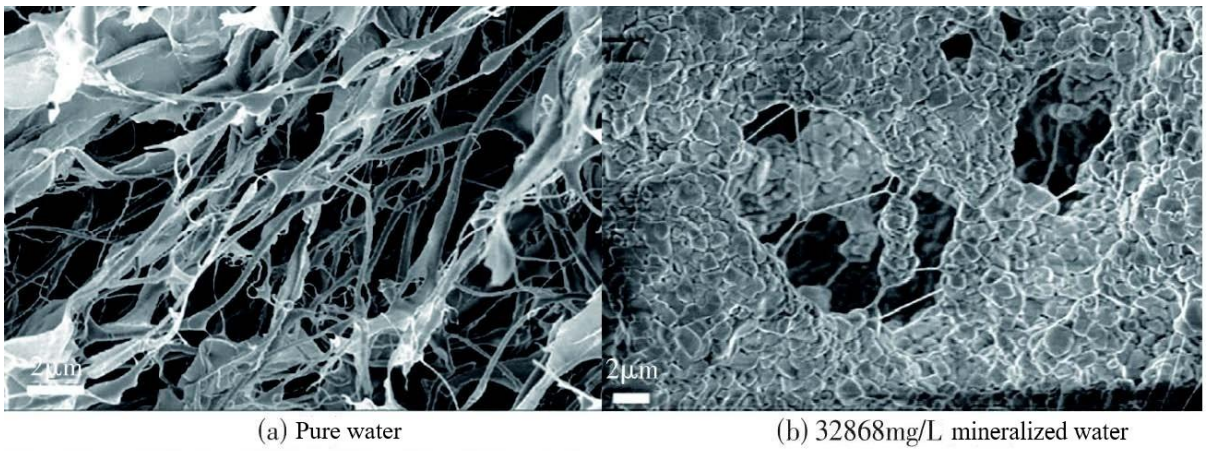

Figure 9 SEM images of PAAA-1 pure aqueous solution and 32868mg/L mineralized aqueous solution

3.4 Viscous Behavior of Copolymer Solutions

3.4.1 Effect of Polymer Solution Concentration on Apparent Viscosity

DOI:

The viscosity-increasing performance of PAAA series polymer solutions is shown in Fig. 10. Fig. 10(a) and (b) show the change in apparent viscosity of PAAA series binary and ternary copolymers in aqueous solution with polymer concentration, tested at 25°C and 85°C, respectively. The apparent viscosity of the polymer increases with increasing polymer concentration. At low polymer concentrations, the number of polymer molecules in the solution is small. At higher copolymer concentrations, the collision rate between molecules is higher. Intra- and intermolecular hydrogen bonding forms a three-dimensional network structure. The electrostatic repulsion of the highly polar groups on AMPS increases the hydrodynamic radius of the macromolecules, macroscopically manifesting as increased apparent viscosity. Fig. 10(c) and (d) show the change in apparent viscosity of PAAA series binary and ternary copolymers in mineralized water with a salinity of 32868 mg/L with polymer concentration, tested at 25°C and 85°C, respectively. It can be seen that as concentration increases, the viscosity of the polymer solution gradually increases, but compared to the apparent viscosity in aqueous solution, it decreases significantly. This is because the addition of complex inorganic salts to the solution causes the polymer macromolecular chains to coil, reducing the apparent viscosity.

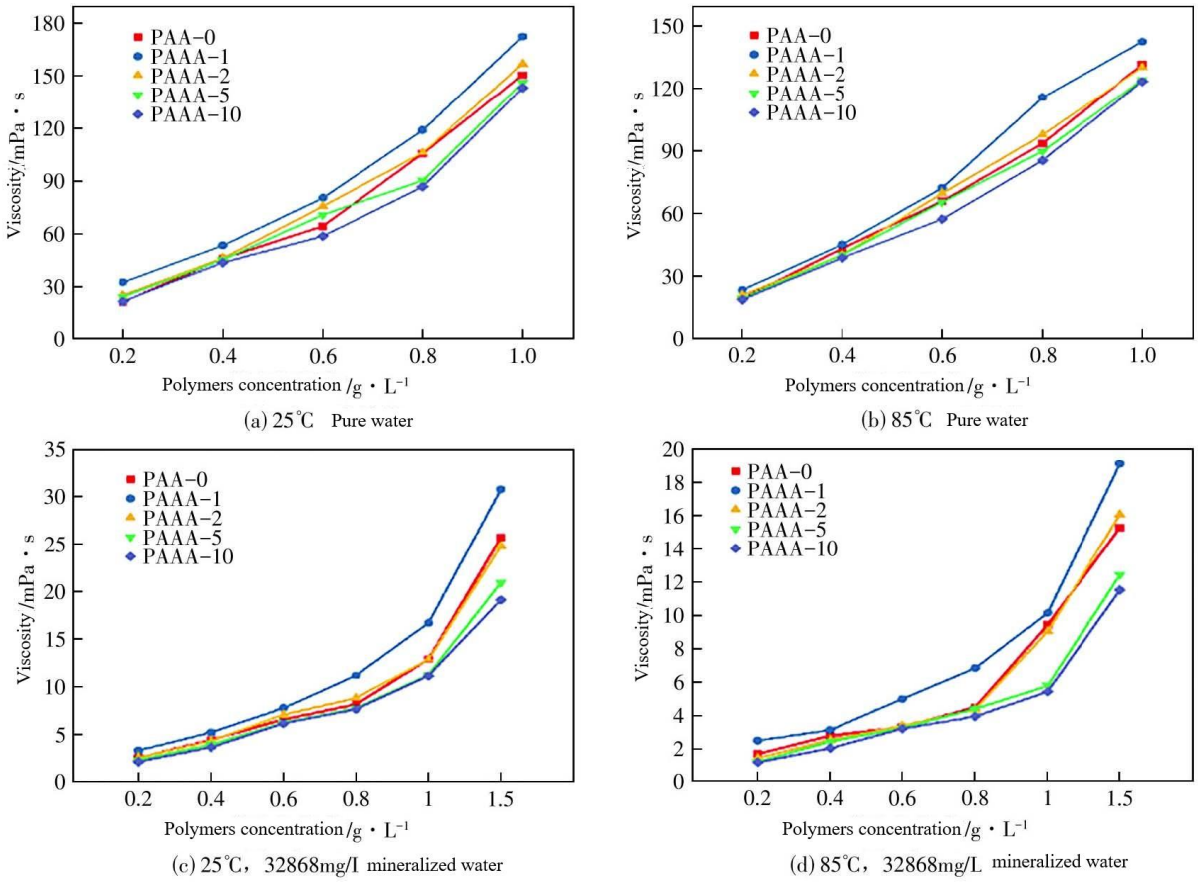

Figure 10 Apparent viscosity of PAAA series polymers at different concentrations

3.4.2 Effect of Temperature on Apparent Viscosity of PAAA System in Aqueous Solution

Fig. 11(a) shows the effect of temperature on the apparent viscosity of the PAAA system in aqueous solution, with a prepared solution concentration of 1000 mg/L. Fig. 11(b) shows the effect of temperature on the apparent viscosity of the polymer PAAA system in mineralized water with 32868 mg/L salinity, tested at a concentration of 1500 mg/L. It is clearly evident from the figures that polymer viscosity gradually decreases as temperature rises. As temperature increases, the thermal motion of the polymer main chains intensifies, entanglements between molecular chains become looser, the hydrodynamic radius decreases, and higher temperatures may induce hydrolysis of the polymer's amide groups, leading to viscosity decrease. From Fig. 11(a), it can be seen that PAAA-1 has the highest apparent viscosity and the best temperature resistance. From Fig. 11(b), it is still evident that PAAA-1's mineralized water solution has the highest apparent viscosity and the best temperature resistance, and

DOI:

is significantly better than the polymer solution without APTAC. This indicates that the introduction of the third monomer successfully increased the polymer's apparent viscosity and enhanced its temperature resistance, which will significantly improve the polymer's oil displacement efficiency. Furthermore, it is clear that the viscosity retention rate of the polymer's apparent viscosity in mineralized water is significantly lower than in pure water. This is because the polymer chains coil in salt solution, and entanglements between chains are fewer than in aqueous solution. As the thermal motion of the main chains intensifies, the network formed by electrostatic interactions and hydrogen bonds is destroyed, and viscosity decreases faster. Therefore, the viscosity retention rate of the polymer's apparent viscosity is lower in mineralized water than in pure water.

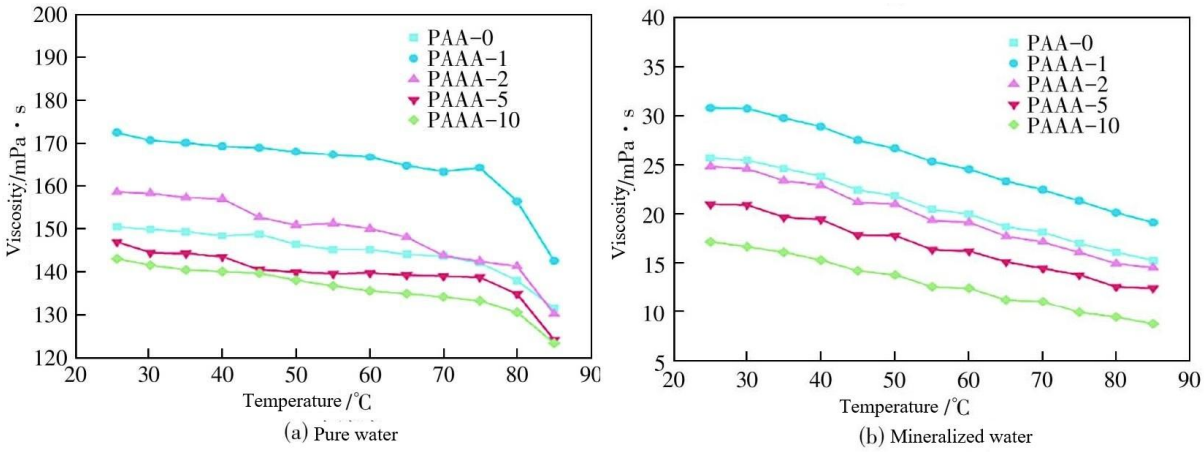

Figure 11 Change in apparent viscosity of PAAA series polymer aqueous solution and mineralized aqueous solution with temperature

3.4.3 Effect of Different Salt Types on Polymer Solution Viscosity

Fig. 12 shows the change in viscosity of polymer solutions with different salt concentrations, all at a polymer concentration of 2000 mg/L. The apparent viscosity of the PAAA-1 ternary copolymer salt solution is higher than that of the PAA-0 binary copolymer, indicating that the introduction of the third monomer has a certain effect. When the concentrations of NaCl, $CaCl_2$, and $MgCl_2$ increase, the apparent viscosity of PAA-0 and PAAA-1 solutions decreases and then tends to level off. This is because salts, as small molecule electrolytes, shield the charges on the ionic groups of the polymer chains, weakening electrostatic repulsion, causing the polymer long chains to coil, reducing the hydrodynamic volume, manifested as viscosity decrease. On the other hand, the addition of salt increases solvent polarity, the electrostatic force of ions disrupts the original water structure, forming water molecule layers, promoting hydration. Furthermore, it can be seen that the ternary copolymer synthesized still has relatively good apparent viscosity in high salt concentration. This is because the ternary copolymer contains a high content of sulfonate, and the existing quaternary ammonium salt structure can interact with amide bonds to form a network structure, enhancing salt resistance, keeping its molecular chain structure in a relatively extended state. Therefore, it can be seen that the polymer solution has good salt resistance, and the ternary copolymer's salt resistance is superior to the binary copolymer.

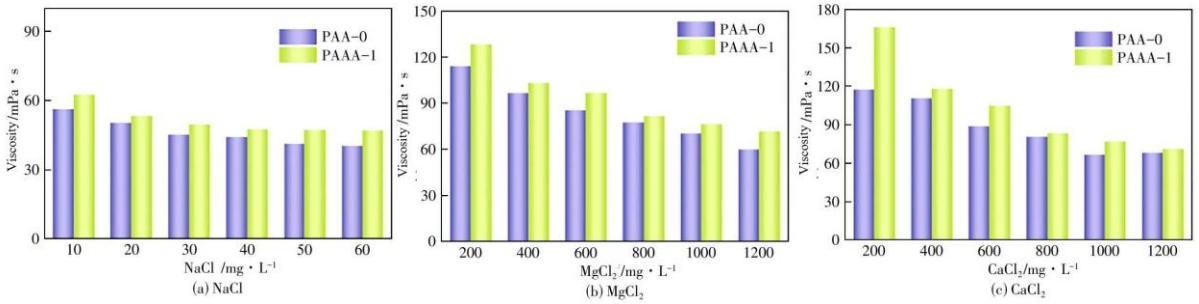

Figure 12 Comparison of viscosity exhibited by PAA-0 and PAAA-1 polymer solutions in NaCl, MgCl2,

and CaCl2 solutions of different concentrations

3.4.4 Effect of Shear Rate on Polymer Solution Viscosity

Shear also affects the oil displacement efficiency of polymers. During injection into the formation and migration within the near-wellbore zone and porous media underground, molecular chains are easily sheared and broken, and entangled structures are also destroyed, causing irreversible viscosity loss. Therefore, shear resistance is also an important requirement for oil-displacing polymers. As shown in Fig. 13, the relationship between the measured viscosity of polyacrylamide copolymer aqueous solutions and shear rate conforms to the power-law equation $\mu = K\gamma^{n-1}$, where μ is the apparent viscosity of the AM-AMPS copolymer in mPa·s; K is the consistency coefficient; γ is the shear rate in s^{-1}; n is the flow behavior index, dimensionless. From the figure, it can be seen that the flow behavior index n of the copolymer aqueous solutions is less than 1, indicating that their aqueous solutions are typical pseudoplastic fluids. Fig. 13 shows solutions all prepared at a concentration of 2000 mg/L. Fig. 13(a) measures the viscosity change with shear rate for 20 million molecular weight PAM, PAA-0, and PAAA-1 at 25°C. It can be seen that the consistency coefficient generally shows an increasing trend, indicating enhanced viscosity-increasing ability of the polymers. Fig. 13(b) measures the viscosity change with shear rate for 20 million molecular weight PAM, PAA-0, and PAAA-1 at 85°C. It can be seen that the consistency coefficients of the polymers decrease significantly at high temperature, but the ternary copolymer is always superior to the binary copolymer.

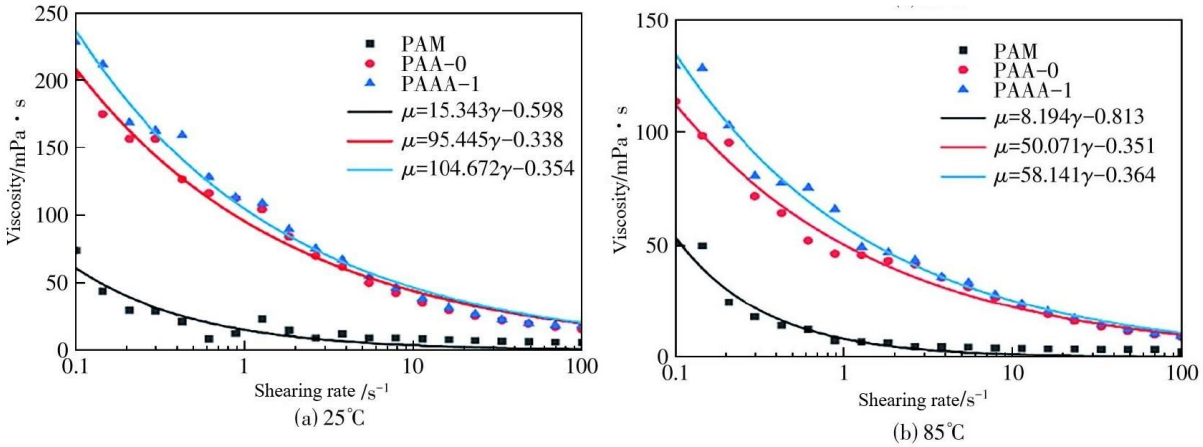

Figure 13 Viscosity variation with shear rate for PAM, PAA-0, and PAAA-1 with a molecular weight of 2000W at 25°C and 85°C

Whether viscosity can recover after high-speed shear is also an important factor in judging polymer oil displacement efficiency. Fig. 14(a) and (b) test the shear recovery performance of 2000 mg/L polymer aqueous solutions at 25°C and 85°C, switching repeatedly between 7.34 s^{-1}, 100 s^{-1}, and 500 s^{-1}. From the figures, it can be seen that after high-speed shear, the apparent viscosity of the polymer eventually recovers completely. This is because the polymer contains a large number of hydrogen bonds and positive-negative ion interactions, which are reversible, thus restoring the molecular structure damaged by shear, exhibiting excellent shear recovery performance. Even at 85°C, PAA-0 and PAAA-1 still have excellent shear recovery performance.

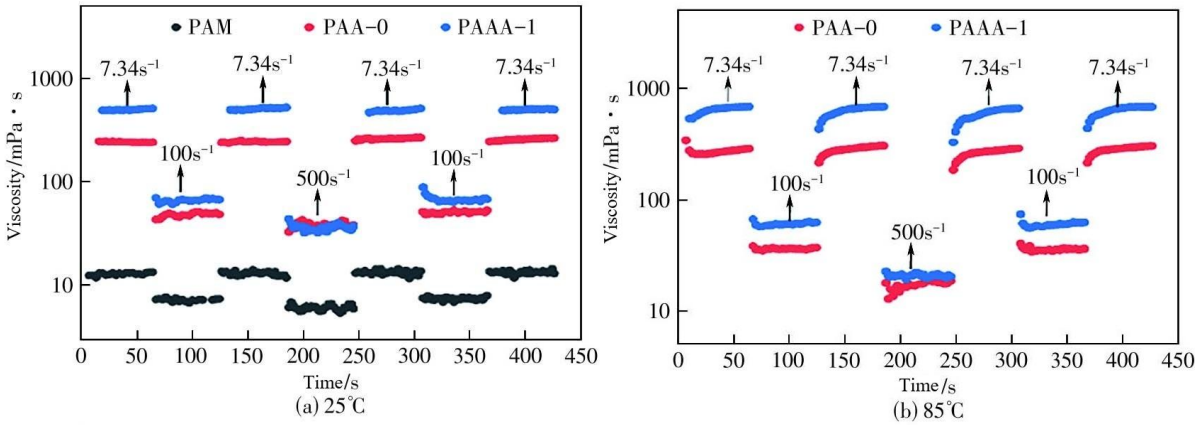

Figure 14 Shear recovery performance of PAM, PAA-0, and PAAA-1 with a molecular weight of 20 million at 25°C and 85°C

4 Conclusion

(1) Using an adiabatic polymerization method, potassium persulfate and organic amine HMTEA were selected as the redox initiator to copolymerize acrylamide, 2-acrylamido-2-methylpropanesulfonic acid, and (3-acrylamidopropyl)trimethylammonium chloride, preparing a water-soluble ternary amphoteric branched polymer. The optimal polymerization conditions were determined as: mass ratio of AM to AMPS 6:4, initiator to total monomer mass ratio 0.02%, APTAC dosage 1% of the total mass of AM and AMPS, optimal initiation temperature 14°C, oxidant to reductant molar ratio 1:1.2, yielding the ternary branched copolymer with optimal performance.

(2) The structure of the amphoteric branched polymer was confirmed by ^{1}H NMR and FTIR. The intrinsic viscosity of the polymers was measured using an Ubbelohde viscometer, and the viscosity-average molecular weight was obtained. The molecular weight of the product obtained under optimal conditions was estimated to reach 27.58 million.

(3) The optimally synthesized polymer PAAA-1, at a dosage of 1500 mg/L in a solution with mineralization of 32868 mg/L and 85°C, had an apparent viscosity of 19.13 mPa·s. Its temperature and shear resistance in brine solution were superior to the binary copolymer PAA-0 of acrylamide (AM) and 2-acrylamido-2-methylpropanesulfonic acid (AMPS), showing promising application prospects in tertiary oil recovery.

References

[1] MING Anqi, LI Xiaoxiao, SUN Jun, et al. The comparison of polymerization activity of typical cationic quaternary ammonium salt monomers[J]. Polymers for Advanced Technologies, 2024, 35(1): e6277.

[2] TIAN Qirui, HAN Peihui, LI Bo, et al. Thermo- and CO2-triggered swelling polymer microgels for reducing water-cut during CO2 flooding[J]. Journal of Applied Polymer Science, 2020, 137(4): 48305.

[3] KO Jiwoo, ZHAO Zhijun, HWANG Soon Hyoung, et al. Nanotransfer printing on textile substrate with water-soluble polymer nanotemplate[J]. ACS Nano, 2020, 14(2): 2191-2201.

[4] TRIGO-LOPEZ Miriam, MUOZ Asuncion, MENDIA Aránzazu, et al. Palladium-containing polymers as hybrid sensory materials (water-soluble polymers, films and smart textiles) for the colorimetric detection of cyanide in aqueous and gas phases[J]. Sensors and Actuators B: Chemical, 2018, 255: 2750-2755.

[5] DUIS Karen, JUNKER Thomas, COORS Anja. Environmental fate and effects of water-soluble synthetic organic polymers used in cosmetic products[J]. Environmental Sciences Europe, 2021, 33(1): 21.

[6] FU Xingqin, ZHANG Yuejun, JIA Xu, et al. Research progress on typical quaternary ammonium salt polymers[J]. Molecules, 2022, 27(4): 1267.

[7] JAEGER Werner, BOHRISCH Joerg, LASCHEWSKY Andre. Synthetic polymers with quaternary nitrogen atoms-Synthesis and structure of the most used type of cationic polyelectrolytes[J]. Progress in Polymer

Science, 2010, 35(5): 511-577.
[8] MIN Jingli. Synthesis and properties of polyacrylamide thermostable and salt-tolerant polymers[D]. Jinan: Shandong University, 2017.
[9] HU Xiaona, YI Zhuo, LIU Xi, et al. Salt tolerance mechanism of acrylamide/sodium acrylate/2-acrylamido-2-methyl-propanesulfonic acid sodium copolymer[J]. Petrochemical Technology, 2024, 53(6): 855-861.
[10] HU Xiaona, YI Zhuo, LIU Xi, et al. Mechanism of temperature resistance of AM/AANa/AMPSNa copolymer based on molecular simulation[J]. Science Technology and Engineering, 2025, 25(1): 157-164.
[11] DENG Bo, LUO Xueqin, JIANG Feng, et al. A weakly cationic temperature tolerant and salt resistant polymer: Synthesis and properties[J]. Macromolecular Research, 2022, 30(8): 579-586.
[12] SUI Yu, CAO Guangsheng, GUO Tianyue, et al. Synthesis and mechanism study of temperature- and salt-resistant amphoteric polyacrylamide with MAPTAC and DTAB as monomers[J]. Processes, 2022, 10(8): 1666.